J Mol Model (2013) 19:2069–2078
DOI 10.1007/s00894-012-1636-4

ORIGINAL PAPER

CO_2 adsorption on polar surfaces of ZnO

Sergio A. S. Farias · E. Longo · R. Gargano · João B. L. Martins

Received: 30 April 2012 / Accepted: 7 October 2012 / Published online: 24 October 2012

Abstract Physical and chemical adsorption of CO_2 on ZnO surfaces were studied by means of two different implementations of periodic density functional theory. Adsorption energies were computed and compared to values in the literature. In particular, it was found that the calculated equilibrium structure and internuclear distances are in agreement with previous work. CO_2 adsorption was analyzed by inspection of the density of states and electron localization function. Valence bands, band gap and final states of adsorbed CO_2 were investigated and the effect of atomic displacements analyzed. The partial density of states (PDOS) of chemical adsorption of CO_2 on the ZnO(0001) surface show that the *p* orbitals of CO_2 were mixed with the ZnO valence band state appearing at the top of the valence band and in regions of low-energy conduction band.

Keywords CO_2 adsorption · Electronic localization function · First principles · Plane wave · ZnO

Introduction

Zinc oxide is a wide *band gap* semiconductor (3.4 eV) [1–4]. The surface features of this oxide are of fundamental importance for numerous technological applications, such as, the electrical behavior of ZnO varistor, sensors and catalysis. From the viewpoint of molecular adsorption over metal oxides, three surfaces of ZnO are of interest: a) (0001) polar surface terminated with Zn atoms, b) $(000\bar{1})$ polar surface terminated with O atoms, and c) the non-polar prism $(10\bar{1}0)$ surface with Zn and O atoms. The (0001) and $(000\bar{1})$ surfaces of single-crystal ZnO are unreconstructed or reconstructed depending upon the surface preparation conditions [5].

Adsorption of CO_2 on ZnO surface is important for environmental detection, and testing for basicity. Moreover, CO_2 is a precursor for the methanol synthesis, which is also associated with defect formation [6–9]. In this case, CO_2 adsorption on $(000\bar{1})$ and nonpolar surfaces was largely studied. The formation of CO_2 anions is energetically favored by charge transfer from the metal upon adsorption, which could lead to the formation of carbon species [10]. Carbon dioxide adsorption on $(10\bar{1}0)$ surface was investigated by means of *ab initio* and semiempirical methods [7–9, 11–14]. DFT showed CO_2 dissociation at oxygen vacancy of $(000\bar{1})$ surface [11]. Tridentate species were reported for polar and nonpolar surfaces from high resolution electron energy loss spectroscopy (HREELS) and other spectroscopic methods [6, 15, 16]. Bidentate species were also experimentally shown for the nonpolar surface [17], while DFT study presented a carboxylate species from carboxylic acids [12]. An angle of 30° between the surface normal and the molecular plane was obtained from near edge X-ray absorption fine structure (NEXAFS) [18]. Quantum mechanics/molecular mechanics (QM/MM) studies indicated that CO_2 upon adsorption on $(000\bar{1})$ surface retains a linear structure [13]. DFT study showed that unidentate structure of a carbon atom interacts with a lattice oxygen atom leading to the formation of carbonate with binding energy of 139.6 kJ.mol^{-1} [14].

S. A. S. Farias (✉) · J. B. L. Martins
Laboratório de Química Computacional, IQ, UnB,
CP 4478,
Brasília, DF 70904-970, Brazil
e-mail: fariassas@gmail.com

E. Longo
INCTMN, Departamento de Físico Química,
Instituto de Química, Unesp,
Araraquara, SP 14800-900, Brazil

R. Gargano
Instituto de Física, UnB,
CP 4455,
Brasília, DF 70919-970, Brazil

On the other hand, the adsorption of CO_2 on polar (0001) surface was scarcely investigated. On the (0001) surface, each zinc cation has a single vacant coordination in relation to the bulk within oxygen anions. This is the requirement for the dissociation of Brønsted acids on acid and basic site pairs of ZnO surfaces [19]. A molecular beam study of CO_2 on (0001) surface showed an adsorption heat of 34 kJ.mol^{-1} [20–22] in agreement with the physisorption heat of 31 kJ.mol^{-1}, while chemisorption of 140 kJ.mol^{-1} was reported for the nonpolar surface [23, 24]. C K-edge near edge X-ray absorption fine structure presents a peak at 290 eV for the (0001) surface and an angle of 68° between surface normal and molecular plane [25]. Low-energy electron diffraction (LEED) analysis showed that CO_2 adsorbs with both carbon and oxygen on (0001) surface [26].

The aim of this work is to investigate theoretically the physical adsorption of CO_2 on the (0001) and $(000\bar{1})$ surfaces, and the chemical adsorption of CO_2 on the (0001) surface. This task was accomplished: a) by evaluating the local structure around the CO_2 on ZnO surfaces, b) through the density of states of adsorption process; c) examining the electronic density between adsorbed and free molecule; d) in addition, comparing between the values of physical and chemical adsorption energies, and also comparing these with the literature values. To achieve these goals, we have used the density functional theory (DFT) [27] to study CO_2 on ZnO. Since the mechanism of stabilization is not well established in periodic calculations of ZnO polar surfaces, we have simulated *slabs* varying the number of layers in order to find a stationary state. Namely, we simulated supercell *slabs* with four, six and eight layers while keeping the surface areas of (0001) and $(000\bar{1})$ fixed.

Computational details

DFT has been largely used to describe the adsorption on surfaces of metal oxides, specifically the structural and electronic properties. Bulk parameters of ZnO were well established using DFT and pseudopotentials [28–32]. Perdew and Wang functional (PW91) [33] using ultrasoft pseudopotential (US-PP), and Perdew-Burke-Ernzerhof (PBE) [34] and PW91 using projector augmented wave (PAW) results are almost identical for simple properties like lattice constant and bulk modulus but not for properties where surface effects are present [35]. Although, US-PP and PAW provide almost equivalent results for the bond lengths and the vibrational stretch frequencies for some molecules, PAW method shows superior to US-PP for energy differences [36]. Therefore, we have used both methods. The positions of the nuclei were relaxed using ultrasoft pseudopotential (US-PP) method to describe the ion-electron interaction with eigenstates expanded in basis functions like plane waves [37], while PAW method was used for property analysis.

Periodic calculations were performed using DFT. Swart and Snijders [38] showed that PBE and PW91 functionals gives almost the same mean errors for bond lengths, and the best-performing exchange-correlation potentials are found to be Becke–Perdew, PBE and PW91. Orita [39] showed that all electron PBE and PW91 adsorption energies and structures give the same trend and almost the same results for CO adsorption. Therefore, the exchange and correlation effects were obtained according to the generalized gradient approximation (GGA) using the PW91 functional [34] implemented in the algorithm of VASP4.6 computational code [40]. The O $2s^2\ 2p^4$, Zn $3d^{10}\ 2s^2$, and C $2s^2\ 2p^2$ were treated as valence states. The atomic positions of CO_2 molecule and ZnO were relaxed with full optimization using the Quasi-Newton algorithm. The energy cutoff was 420 eV, and the K points mesh was 3×3×3 in the first Brillouin zone. All forces were converged with criteria less than 0.20 eV/Å per atom.

ZnO crystallizes in a structure of *B*4 type (wurtzite) of $P6_3mc$ space group [41]. The experimental lattice parameters values are a=3.2495 Å and c=5.2069 Å, and the internal parameter is z=0.3825 Å [42]. In this work we have studied *slabs* of ZnO of four, six and eight layers (Fig. 1) with $(ZnO)_{32}$, $(ZnO)_{48}$ and $(ZnO)_{64}$ units, respectively. The overlayer structures on (0001) and $(000\bar{1})$ surfaces for carbon of CO_2 were described using Wood's notation of (2×2) surface. The adsorbate coverage was $\theta = 1/8$ for these structures. The (0001) surface area was 74.94 Å^2 for all supercell *slabs*. This value was chosen in order to minimize the dipole moment of the *slab*. A vacuum of 10 Å along the z axis was also used.

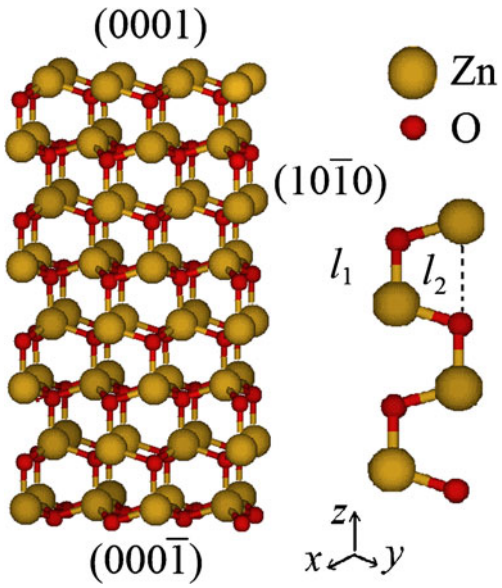

Fig. 1 ZnO slab used for first principles calculations

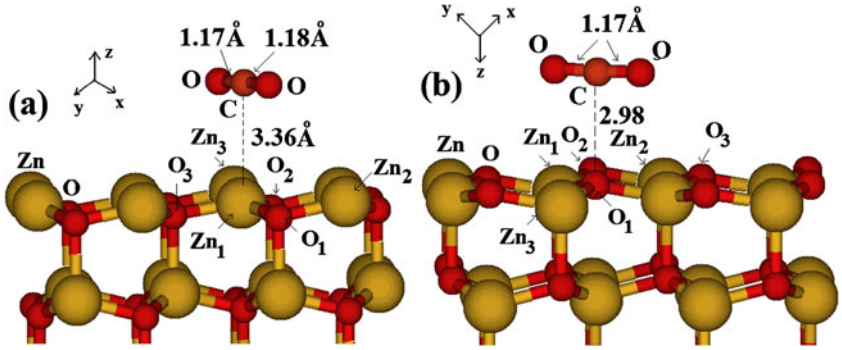

Fig. 2 **a** CO_2 physical adsorption on (0001) and **b** $(000\bar{1})$ surfaces. Only the atoms that are close to adsorbed CO_2 molecule are numbered

Another point of interest of this work was to analyze the adsorption of CO_2 by means of total and partial densities of electronic states (DOS). We have evaluated the energies of physical and chemical adsorptions, valence bands, *band gap*, states of CO_2, and final filled states due to atomic displacements. Electron localization function (ELF) analysis was performed using the DGRID program [43].

Results and discussion

Structure of slabs

Lattice parameters optimized for physical and chemical adsorptions were: a=3.224 Å and c=5.241 Å, in accordance to the experimental values [41, 44]. A vacuum space of approximately 10.00 Å was used in the c direction. These lattice parameters produced a distance of 1.996 Å for the Zn-O bonding close to the experimental distance [41].

There are difficulties in performing calculations of periodic polar surfaces of metal oxides, e.g., NiO, the Cr_2O_3, and Fe_2O_3, mainly due to the instabilities of these surfaces [5]. The stability of polar surfaces is a challenging task not completely understood [45–47]. Several materials have polar surfaces that are stabilized by mechanism of reconstruction or the presence of adsorbates [5, 48]. However, Wander and Harrison [48] showed that polar surfaces of ZnO were not stabilized by water dissociation. ZnO was believed to form unreconstructed polar surfaces [49], while there is evidence of missing Zn ion on the (0001) surfaces [50]. Therefore, Meyer [49] concluded that only charge transfer between polar surfaces can explain the polar termination stability. In this sense, polar surface was stabilized due to rearrangement of electronic structure of polar surfaces [47], although charge transfer mechanism should result in a metallic surface state formation [45, 51]. Otherwise the stabilization mechanism is dependent on the preparation conditions [52] and polar surfaces of very small oxide particles could be stable [45]. From ionic model a macroscopic field perpendicular to the surface induces the energy to diverge with slab thickness [47]. Therefore, it was expected that CO_2 adsorption could stabilize the surface.

The surface energies for four, six and eight layers were calculated to study the influence of slab thickness using the following equation:

$$E_{surf} = [E_{slab} - n.E_{bulk}]/2A, \quad (1)$$

where E_{slab} is the relaxed slab energy, E_{bulk} is the bulk energy, n is the number of layers, and A is the surface area.

The results for the surface energies are 2.32 J/m^2 in the case of four layers, and 1.60 J/m^2 for six and eight layers. However, the structure of four layers slab is completely distorted compared to the relaxation of six and eight layers, which jointly with this large surface energy suggests that the four layers slab is not stable. Otherwise, the energies of six and eight layers suggest

Table 1 Displacement differences (Å) of Zn and O atoms between (0001) and $(000\bar{1})$ surface layers for the physical adsorption

(a)	X	Y	Z
Zn_1	0.001	0.000	0.280
Zn_2	0.007	0.002	0.204
Zn_3	−0.001	0.007	0.210
Zn_4	−0.002	0.002	0.205
Zn_5	0.003	0.001	0.209
Zn_6	−0.001	0.003	0.210
Zn_7	0.004	0.003	0.214
Zn_8	−0.003	0.002	0.221
O_1	0.013	0.000	−0.251
O_2	0.012	0.007	−0.301
O_3	0.001	0.001	−0.312
O_4	0.005	0.002	−0.308
O_5	0.004	0.002	−0.310
O_6	0.005	0.003	−0.310
O_7	0.008	0.006	−0.325
O_8	0.006	−0.002	−0.328

(a) Atoms 1, 2 and 3 are close to CO_2 molecule, while atoms 4, 5, 6, 7, and 8 are the remaining atoms of the same layer (See Fig. 2) in order of distance from CO_2 molecule

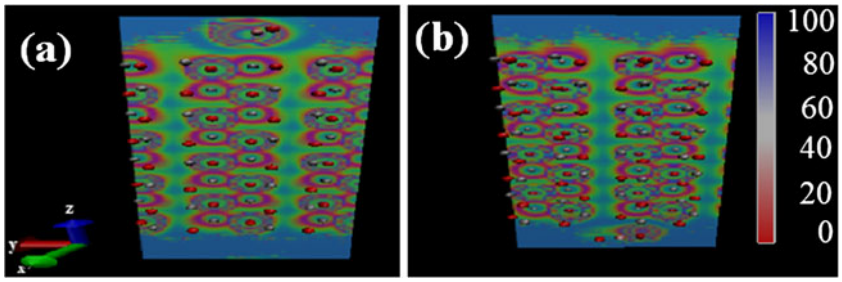

Fig. 3 ELF (0.8) for the physical adsorption on **a** (0001) and **b** $(000\bar{1})$ layers

that only slabs with more than four layers should be used for the adsorption study. These surface energies are in agreement with the values found in the analyses of $(10\bar{1}0)$ and $(11\bar{2}0)$ surfaces [3].

CO_2 physical adsorption on (0001) and $(000\bar{1})$ surfaces

We investigated the adsorption energy (E_{ads}) of CO_2 on ZnO (0001) surface using the following equation:

$$E_{ads} = -(E_{slab+sub} - E_{slab} - E_{sub}), \quad (2)$$

where $E_{slab\ +\ sub}$ is the total energy of the adsorbate-substrate complex, E_{slab} is the bare surface total energy, and E_{sub} is the total energy of isolated CO_2 molecule. These values are of interest for the water-gas shift reactions and the methanol synthesis. The adsorption energies of CO_2 on (0001) and $(000\bar{1})$ ZnO surfaces are 6.7 kJ.mol^{-1}, and 11.9 kJ.mol^{-1}, respectively. This is in agreement with the sublimation heat of CO_2 and the physical heat of adsorption of almost 31 kJ.mol^{-1} on ZnO [20–22].

The geometry optimization results for the CO_2 physical adsorption on (0001) and $(000\bar{1})$ surfaces are shown in Fig. 2. The distance between CO_2 molecule and the ZnO surface is shown to be large. In general, dispersion terms are important for an accurate description of this physical adsorption and geometry. However, this large distance is in accordance with the physical process. Besides the influence of the dipole (for polar surfaces), the CO_2 interaction contributes to the atom displacements on the (0001) and $(000\bar{1})$ surfaces. There was an elastic deformation along the slab z axis. The surface relaxation with adsorbed CO_2 molecule showed l_1 and l_2 distances (see Fig. 1) of approximately 2.00 and 3.23 Å, respectively. The optimized structures presented atom displacements for both surfaces, especially the atoms close to adsorbed CO_2 molecule. Slabs showed a large rearrangement of surface atoms when relaxed with less than six layers and the same surface area. However, the parameters obtained for the six and eight layer models kept *B*4 phase symmetry of ZnO during the relaxation of atomic positions. This suggests that the parameters used in these slabs allowed charges to rearrange into the layers of (0001) and $(000\bar{1})$ surfaces. This type of behavior is consistent with the reported physisorption process.

Table 1 shows the displacement differences between (0001) and $(000\bar{1})$ surface layers of three Zn and O atoms close to the CO_2 molecule, plus the five remaining Zn and O atoms of the same layer. Zn and O atoms were identified in order of increasing Zn-C distance. Table 1 shows that the surface rumples. The first three Zn and O atoms closest to CO_2 had approximately the same x and y displacement on (0001) and $(000\bar{1})$ surfaces for all atoms. This statement is in agreement with the expected physisorption behavior.

Internal Zn–O double-layer separations (d_I) were reduced by 48 and 54 % for the CO_2 adsorption on (0001) and

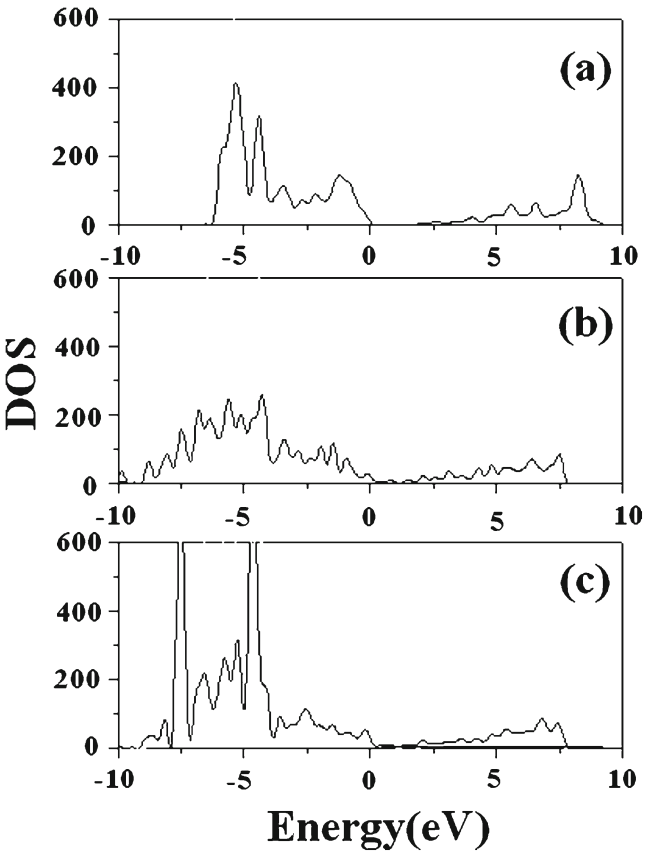

Fig. 4 Total DOS calculated for the **a** bulk on the physical adsorption of CO_2, above **b** (0001) and **c** $(000\bar{1})$ surfaces. The Fermi energy passes through zero eV

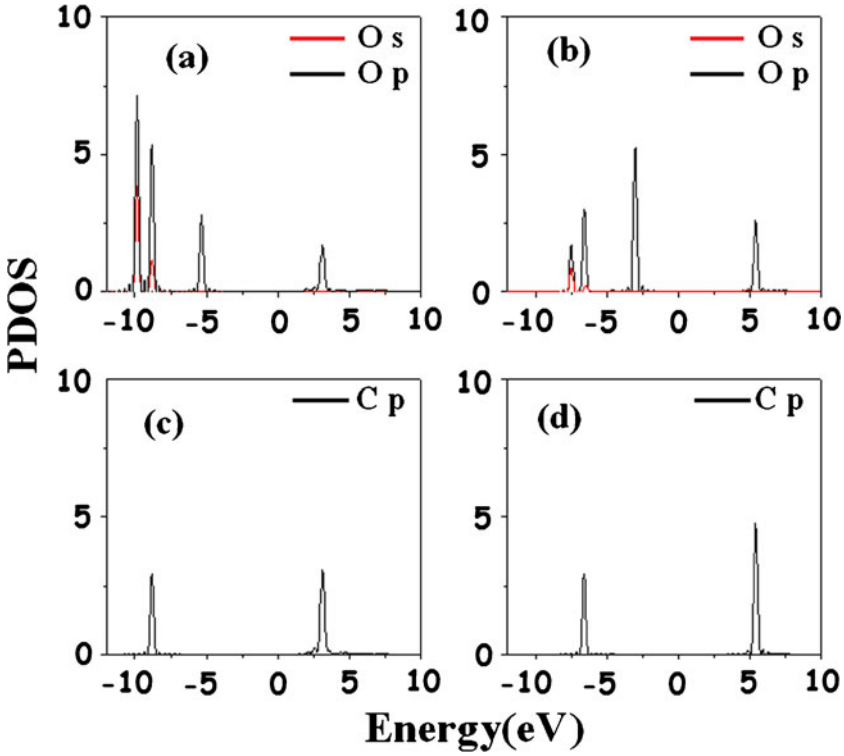

Fig. 5 PDOS calculated for the physical adsorption for the O atom of CO_2 molecule on **a** (0001) and **b** $(000\bar{1})$ surfaces; while for the C atom of CO_2 molecule on **c** (0001) and **d** $(000\bar{1})$ surfaces. The Fermi energy passes through zero eV

$(000\bar{1})$ surfaces, respectively. This is in agreement with the values found earlier for the bare relaxed surface using *ab initio* calculations [53].

Figure 3 shows the ELF analysis of the electronic density using the visual molecular dynamics (VMD) program [54], for the physical adsorption on (0001) and $(000\bar{1})$ surfaces at ELF value of 0.8. Figure 3 indicates that Zn and O bonding is in the ionic-covalent borderline. There is no isoline between CO_2 and (0001) and $(000\bar{1})$ surfaces caused by the CO_2 molecule. This behavior also supports the expected physical adsorption.

Figure 4 shows the total density of states (DOS) for physical adsorption on eight layers model. The electronic structure for the eight layers model is in agreement with the full-potential linear muffin-tin method [55]. The basic difference between the bare (Fig. 4a) and CO_2 covered surface (Fig. 4b and c) is the presence of states located in fundamental *gap* of adsorbed system. This is due to abrupt change in external potential that the electrons feel in surface [56], so there is a slightly negative net charge only on the surface [56].

Analysis of occupied states was conducted through the partial density of states (PDOS). Figure 5 shows the PDOS for CO_2 adsorption on eight layers model on (0001) and $(000\bar{1})$ surfaces. Figure 5a and b are for the O atom, while Fig. 5c and d are for the C atom. For the (0001) surface, the *p* states of O from CO_2 are localized in the region ranging from −10 to −5 eV. In both cases there are no states of CO_2 at the top of the valence band, which is dominated by *p* states of O (ZnO), and it hybridizes with a small amount of *d*

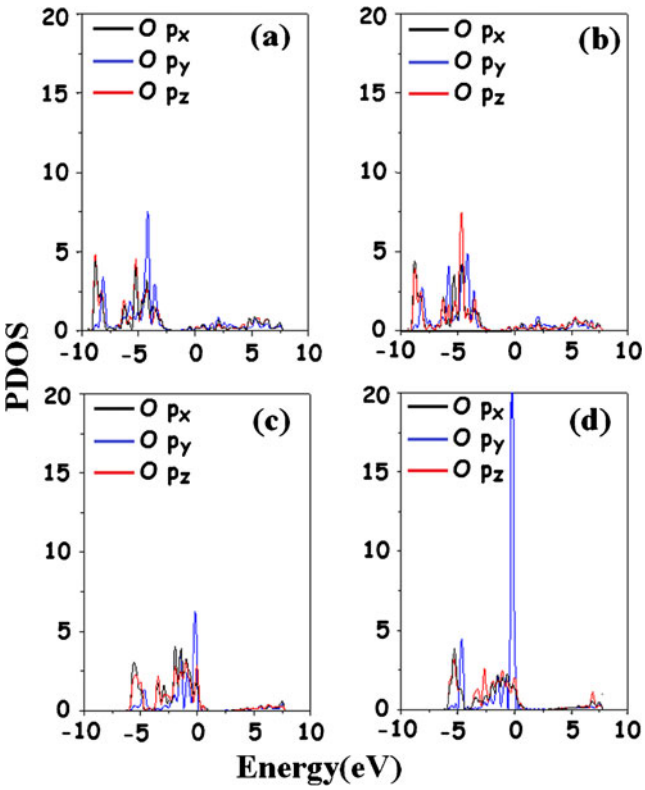

Fig. 6 PDOS for the O atom from most inner layer for adsorption **a** on (0001), and **b** $(000\bar{1})$ surfaces; while for the O atom from top layer for adsorption **c** on (0001), and **d** $(000\bar{1})$ surfaces. The Fermi energy passes through zero

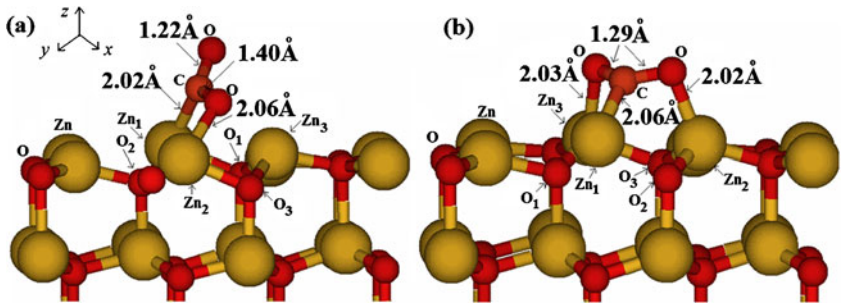

Fig. 7 **a** Chemical adsorption of CO_2 over (0001) surface with bidentate and **b** tridentate configurations

states of Zn. Another difference was found in the valence band due to states occupied by CO_2. Our results are in agreement with experiments using X-ray photoelectron spectroscopy that investigated the physical adsorption [57], and found states filled by CO_2 in the lower energy regions.

Figure 6 shows the *p* orbitals of O atoms for the adsorption on (0001) (Fig. 6a and c) and $(000\bar{1})$ (Fig. 6b and d) surfaces. Figure 6a and b show the contribution of O *p*-orbitals from the middle of the slab, i.e., the inner layers, while Fig. 6c and d depict the O p-orbitals from the top layer. The inner most layers should describe the same behavior as the bulk. Therefore, the *p*-orbitals of top layer are displaced compared to the bulk (Fig. 6). The occupied p_z orbitals are strongly localized on $(000\bar{1})$ surface. This displacement found for O *p*-orbital is in agreement with other theoretical results [53], which exhibit a large peak close to the fermi level on the oxygen atom of $(000\bar{1})$ surface.

Chemical adsorption of CO_2 on (0001) surface with formation of bidentate and tridentate species

Studies using infrared spectroscopy suggest that the interaction of the three centers of CO_2 molecule (tridentate) with the ZnO surface is responsible for methanol synthesis and water-gas-shift reaction [15, 58]. Semi-empirical and *ab initio* calculations as well as experimental data showed a stable bidentate interaction of CO_2 molecule with ZnO surface [6–9, 12, 17, 25, 59]. Therefore, chemical adsorption of CO_2 was studied at (0001) surface, with bidentate and tridentate species. There is no significant difference among results of geometry optimization, electronic density and adsorption energy using six and eight layer models of (0001) surface, and only the eight layer model results are described.

Geometry optimizations for the eight layers model (Fig. 7) give oxygen-carbon distance of 1.40 Å for carbon bidentate species, and 1.29 Å for tridentate. Besides this main difference that suggests a dissociation of bidentate species, the geometry of CO_2 molecule is approximately the same.

Table 2 shows the displacement of three Zn atoms, and three O atoms closest to CO_2 molecule on (0001) surface. Zn closest to C (Zn_1) was displaced significantly in relation to z-axis. The z-axis displacements of chemical adsorption types are opposed to those directions of displacements in physical adsorption. Therefore, displacements in the surface atoms are due to the chemically adsorbed CO_2 molecule, while for the physical adsorption displacements are due to the surface relaxation.

ELF analysis for the chemical adsorption with bidentate and tridentate species (Fig. 8) indicates a covalent bonding between CO_2 and the (0001) surface in both adsorptions. In contrast to the physical adsorption, ELF shows a clear interaction between the CO_2 molecule and the surface for chemical adsorption.

PDOS for chemical adsorption (Fig. 9) also indicates states in the gap as found in Fig. 5 for the physical adsorption. The *p*-filled states of C and O of CO_2 were distributed throughout the valence band, in agreement with the experimental results [57]. In both cases there are depletions of C and O *p* states in the band gap and low-energy of conduction band. Tridentate interaction shows the same PDOS for the two O atoms (Fig. 9b and d), which suggests the same interaction for these two oxygens, while as expected, the bidendate interaction has different PDOS for the two oxygen atoms (Fig. 9a and c).

Plane wave adsorption energy of CO_2 bidentate species is 407.8 kJ.mol^{-1}. This value is smaller than those obtained by

Table 2 Shift (Å) of nearest Zn and O atoms to CO_2 on (0001) surface for chemical adsorption with bidentate and tridentate species (see Fig. 2 for the notation)

	Bidentate			Tridentate		
	X	Y	Z	X	Y	Z
Zn_1	−0.025	−0.002	0.327	0.039	0.050	0.270
Zn_2	0.104	0.093	0.065	−0.041	−0.061	0.046
Zn_3	−0.202	−0.136	0.044	−0.079	−0.010	0.041
O_1	0.017	−0.143	−0.156	−0.025	−0.015	−0.111
O_2	−0.050	−0.111	−0.032	−0.020	−0.059	−0.118
O_3	0.096	0.026	0.180	−0.043	−0.095	−0.024

Atom notations are in order of increasing distance from the C center

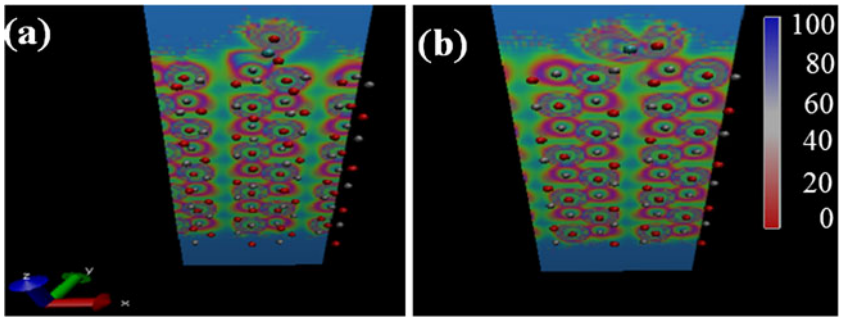

Fig. 8 ELF (0.8) for the chemical adsorption on (0001) surface **a** bidentate and **b** tridentate

Martins and co-workers using semiempirical AM1, and *ab initio* Hartree-Fock method with 3-21G* basis set (RHF/3-21G//AM1) with cluster models [9]. One main advantage of using plane wave basis set is in relation to the basis set superposition error (BSSE), which must be accounted for in the LCAO based methods. The results for cluster models

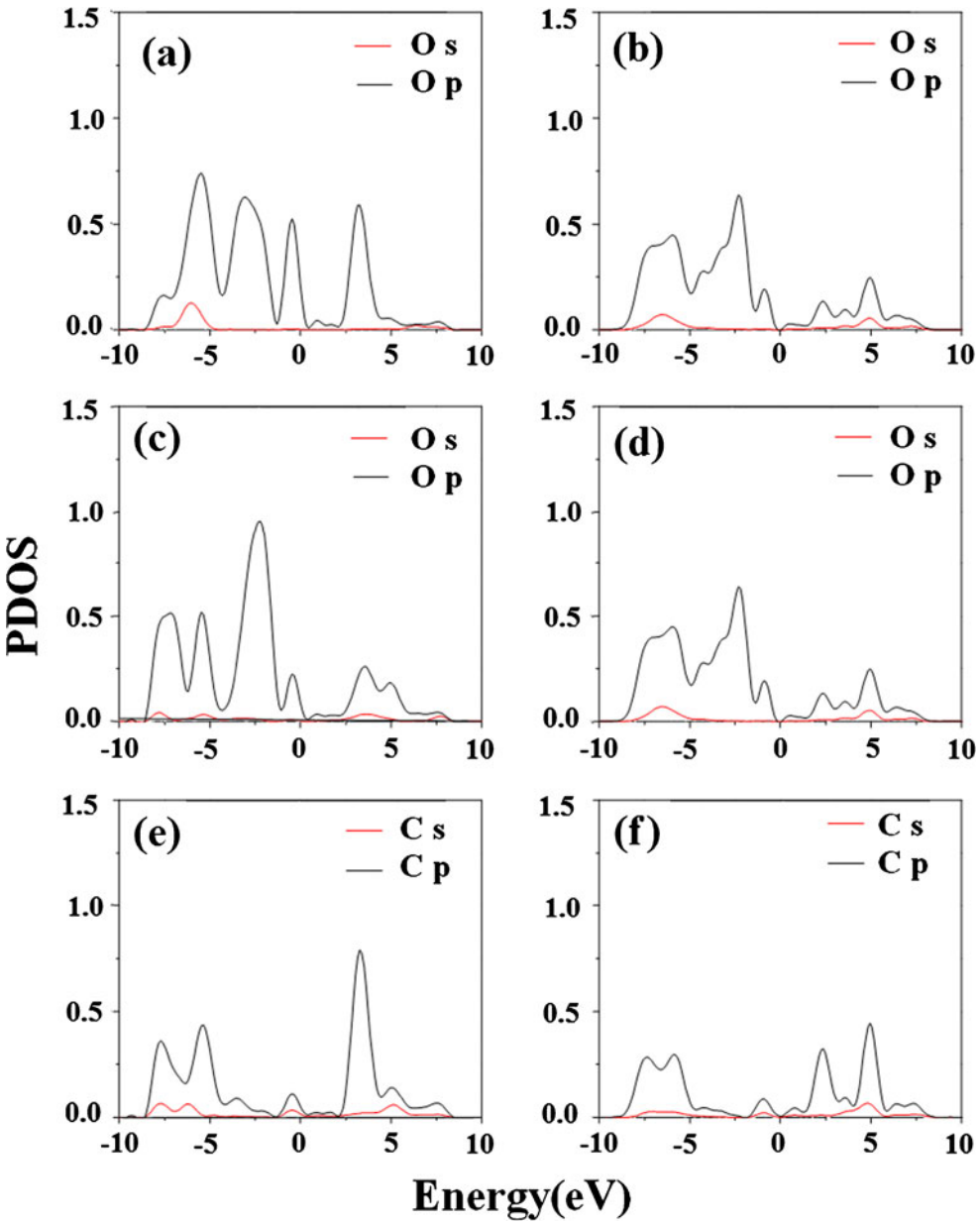

Fig. 9 PDOS calculated for chemical adsorption of CO_2 on (0001) surface, with bidentate and tridentate configurations. For the first oxygen of CO_2 on **a** bidentate and **b** tridentate, for the second oxygen on **c** bidentate and **d** tridentate. For carbon atom of **e** bidentate and **f** tridentate adsorption. The Fermi energy passes through zero eV

have no implicit periodicity, while the importance of periodic conditions is clear for such solid systems. Therefore, it was expected that periodic plane wave results were in better agreement with experimental data.

Table 3 shows a comparison between adsorption of CO_2 tridentate species of the current study and the results of atom-centered basis set of Chuasiripattana on ZnO (0001) surface [58], with adsorption energy in the borderline of physical adsorption. The interatomic distances of this work are in agreement with the reported (2×2) supercell [58]. However, the results for adsorption energies are not in agreement with the previous theoretical study of (2×2) unit cell [58]. At low coverage (1/9ML), the adsorption energy calculated in a (3×3) unit cell is 108.1 kJ.mol^{-1} [58]. Heat of adsorption for the tridentate species on oxygen terminated $(000\bar{1})$ surface was calculated to be 139 kJ.mol^{-1} using PBE functional with cluster model [60]. Carbon dioxide is held on zinc oxide with energies from 108.8 to 154.8 kJ.mol^{-1} [61]. The experimental heat of adsorption for the pristine sites amounts to 34.0 kJ.mol^{-1} for the (0001) surface [22]. This is slightly larger than the value reported for the physisorption of CO_2 of 31 kJ.mol^{-1} by Goepel et al. [23]. Heats of adsorption of 140 kJ.mol^{-1} for CO_2 chemisorption has been reported on nonpolar ZnO surfaces [23]. Chuasiripattana and co-coworkers [58] have used a numerical atom-centered basis set with PBE, with lattice parameters of a=3.302 Å and c=5.317 Å larger than experimental values, while we have used PW91. It is well known that these functionals lead to the difference in interaction energies [35]. Therefore, this difference is partially due to exchange correlation functional and the number of layers used, since there is no significant difference of our structure in relation to the reported data [58].

Conclusions

In this work we carried out CO_2 adsorption study on polar surfaces of ZnO using US-PP and PAW methods. We investigated the structural and electronic properties of physical and chemical adsorption with focus on adsorption energies, and defined the minimum number of layers needed for the adsorption study. The atom positions were fully relaxed.

The surface energy suggests that the *slabs* with more than four layers were needed to study the adsorption process. Zn–O double-layer separation (d_I) has been reduced to 48 and 54 % due to CO_2 adsorption on (0001) and $(000\bar{1})$ surfaces, respectively, which is in agreement with the literature. ELF showed no isoline between CO_2 and (0001) and $(000\bar{1})$ surfaces. Therefore, as expected CO_2 molecule had insignificant interaction with surfaces (0001) and $(000\bar{1})$ in physical adsorption. However, the atoms of double layer are displaced due to relaxation of atomic positions, showing an elastic deformation along the slab z axis.

For the physical adsorption, there were no states of CO_2 at the top of the valence band, which was dominated by p states of O (from ZnO), and it hybridized with a small amount of d states of Zn. The inner most layers should describe the same behavior as the bulk from the PDOS of physical adsorption. Our results are in agreement with experiments using X-ray photoelectron spectroscopy that investigated the physical adsorption, and found states filled by CO_2 in the lower energy regions.

The directions of the displacements on the z-axis, in chemical adsorption types, were opposed to those directions of the displacements in physical adsorption. This shows that the displacements in the surface were related to the chemically adsorbed CO_2 molecule, while in the physical adsorption they were from the relaxation process of surface. One main advantage of using plane wave basis set is in relation to the BSSE. In addition, comparing our chemical adsorption results with cluster models showed the importance of periodic conditions for such solid systems.

ELF for the chemical adsorption with bidentate and tridentate showed a clear interaction between the CO_2 molecule and the surface. The interatomic distances of this work were in agreement with the results of literature. However, the results for adsorption energy were not in agreement with early theoretical study, which showed interaction energy smaller than the expected for this chemical adsorption, in the borderline of physical adsorption. The PDOS completes the visualization of chemical adsorption of CO_2 on (0001) surface, and showed that the p orbitals of CO_2 are distributed throughout the valence band and fundamental *gap*. The p orbitals of CO_2 appeared at the top of the valence band, and in regions of low-energy conduction band.

Table 3 Comparison between the theoretical results of adsorption energy of CO_2 with tridentate (see Fig. 2 for the notation)

	This work	Ref. [58][a]
E_{ads} (kJ.mol^{-1})	−396.9	−55.0
O - Zn_2 (Å)	2.02	2.07
O - Zn_3 (Å)	2.03	2.07
C – Zn (Å)	2.06	2.06
C_{CO2}-$Zn_{(0001)}$ (Å)	1.52	1.41
O_{CO2}-$Zn_{(0001)}$ (Å)	1.85	1.89
O_{CO2}-$Zn_{(0001)}$ (Å)	1.85	1.89

[a]The geometrical parameters and adsorption energy were reported for the (2×2) unit cell

Acknowledgments The authors acknowledge the careful reading done by the referees. The authors are indebted to the financial support of National Council of Technological and Scientific Development (CNPq), Coordenação de Aperfeiçoamento de Pessoal de Nível Superior (CAPES), and National Institute of Science and Technology of Materials in Nanotechnology (INCTMN).

References

1. Abe K, Banno Y, Sasayama T, Koizumi K (2009) J Vac Sci Technol B 27:1652–1654. doi:10.1116/1.3089374
2. Beltran A, Andres J, Calatayud M, Martins JBL (2001) Theoretical study of ZnO (10(1)over-bar-0) and Cu/ZnO (10(1)over-bar-0) surfaces. Chem Phys Lett 338:224–230. doi:10.1016/S0009-2614(01)00238-X
3. Marana NL, Longo VM, Longo E, Martins JBL, Sambrano JR (2008) Electronic and structural properties of the (10(1)over-bar0) and (11(2)over-bar0) ZnO surfaces. J Phys Chem A 112:8958–8963
4. Tabatabaei J, Sakakini BH, Waugh KC (2006) On the mechanism of methanol synthesis and the water-gas shift reaction on ZnO. Catal Lett 110:77–84
5. Noguera C (2000) Polar oxide surfaces. J Phys Condens Matter 12: R367–R410
6. Noei H, Woll C, Mahler M, Wang YM (2011) Activation of carbon dioxide on ZnO nanoparticles studied by vibrational spectroscopy. J Phys Chem C 115:908–914. doi:10.1021/jp102751t
7. Martins JBL, Longo E, Salmon ODR, Espinoza VAA, Taft CA (2004) The interaction of H-2, CO, CO2, H2O and NH3 on ZnO surfaces: an Oniom study. Chem Phys Lett 400:481–486
8. Martins JBL, Longo E, Taft CA (1998) CO2 and NH3 interaction with ZnO surface: An AM1 study. Int J Quantum Chem 70:367–374
9. Martins JBL, Sambrano JR, Vasconcellos LAS, Longo E, Taft CA (2004) Theoretical analysis of the interaction of CO, CO2, and NH3, with ZnO. Quim Nova 27:10–16
10. Borodko Y, Somorjai GA (1999) Catalytic hydrogenation of carbon oxides—a 10-year perspective. Appl Catal A Gen 186:355–362
11. Fink K (2006) Ab initio cluster calculations on the electronic structure of oxygen vacancies at the polar ZnO(0001) surface and on the adsorption of H-2, CO, and CO2 at these sites. Phys Chem Chem Phys 8:1482–1489
12. Moreira NH, da Rosa AL, Frauenheim T (2009) Covalent functionalization of ZnO surfaces: a density functional tight binding study. Appl Phys Lett 94:193109
13. French SA, Sokol AA, Bromley ST, Catlow CRA, Rogers SC, King F, Sherwood P (2001) From CO2 to methanol by hybrid QM/MM embedding. Angew Chem Int Ed 40:4437–4440. doi:1433-7851/01/4023-4438
14. Chen WK, Zhang YF, Ding KN, Xu YJ, Li Y, Li JQ (2004) A density functional theory study of the adsorption of CO2 on a ZnO (10(1)over-bar0) surface. Chin J Struct Chem 23:337–341
15. Wang Y, Kovacik R, Meyer B, Kotsis K, Stodt D, Staemmler V, Qiu H, Traeger F, Langenberg D, Muhler M, Woll C (2007) CO2 activation by ZnO through the formation of an unusual tridentate surface carbonate. Angew Chem Int Ed 46:5624–5627. doi:10.1002/anie.200700564
16. Kotsis K, Stodt D, Staemmler V, Kovacik R, Meyer B, Traeger F, Langenberg D, Strunskus T, Kunat M, Woll C (2008) CO2 adlayers on the mixed terminated ZnO(10-10) surface studied by he atom scattering, photoelectron spectroscopy and ab initio electronic structure calculations. Z Phys Chem Int J Res Phys Chem Chem Phys 222:891–915
17. Davis R, Walsh JF, Muryn CA, Thornton G, Dhanak VR, Prince KC (1993) The orientation of formate and carbonate on Zno[10(1)over-Bar0]. Surf Sci 298:L196–L202
18. GutierrezSosa A, Crook S, Haq S, Lindsay R, Ludviksson A, Parker S, Campbell CT, Thornton G (1996) Influence of Cu overlayers on the interaction of CO and CO2 with ZnO(000(1)over-bar)-O. Faraday Discuss 105:355–368
19. Barteau MA (1993) Site requirements of reactions on oxide surfaces. J Vac Sci Technol A 11:2162–2168
20. Wang J, Burghaus U (2005) Adsorption of CO on the copper-precovered ZnO(0001) surface: a molecular-beam scattering study. J Chem Phys 123(18):184716
21. Wang J, Burghaus U (2005) Structure-activity relationship: the case of CO2 adsorption on H/Zn-ZnO(0001). Chem Phys Lett 403:42–46
22. Wang J, Burghaus U (2005) Adsorption dynamics of CO2 on Zn-ZnO(0001): a molecular beam study. J Chem Phys 122:044705
23. Göpel W, Bauer RS, Hansson G (1980) Ultraviolet photoemission studies of chemisorption and point defect formation on ZnO nonpolar surfaces. Surf Sci 99:138–156. doi:10.1016/0039-6028(80)90584-1
24. Hotan W, Göpel W, Haul R (1979) Interaction of CO2 and co with nonpolar zinc oxide surfaces. Surf Sci 83:162–180. doi:10.1016/0039-6028(79)90486-2
25. Gutierrez-Sosa A, Evans TM, Parker SC, Campbell CT, Thornton G (2002) Geometry of C1-3 oxygenates on ZnO(0001)-Zn. Surf Sci 497:239–246. doi:10.1016/S0039-6028(01)01645-4
26. Cheng WH, Kung HH (1982) Interaction of Co, Co2 and O2 with non-polar, stepped and polar Zn surfaces of Zno. Surf Sci 122:21–39
27. Hohenberg P, Kohn W (1964) Inhomogeneous electron gas. Phys Rev B 136:B864–B871
28. Zhang FY (2011) A possible new transition path for ZnO from B4 to B1. Physica B 406:3942–3946
29. Ashrafi A, Jagadish C (2007) Review of zincblende ZnO: stability of metastable ZnO phases. J Appl Phys 102:071101
30. Charifi Z, Baaziz H, Reshak AH (2007) Ab-initio investigation of structural, electronic and optical properties for three phases of ZnO compound. Phys Status Solidi B Basic Solid State Phys 244:3154–3167
31. Hill NA, Waghmare U (2000) First-principles study of strain-electronic interplay in ZnO: stress and temperature dependence of the piezoelectric constants. Phys Rev B 62:8802–8810
32. Schroer P, Kruger P, Pollmann J (1993) 1st-principles calculation of the electronic-structure of the wurtzite semiconductors Zno and Zns. Phys Rev B 47:6971–6980
33. Perdew JP (1991) Electronic structure of solids. Akademie, Berlin
34. Perdew JP, Burke K, Ernzerhof M (1996) Generalized gradient approximation made simple. Phys Rev Lett 77:3865–3868
35. Mattsson AE, Armiento R, Schultz PA, Mattsson TR (2006) Nonequivalence of the generalized gradient approximations PBE and PW91. Phys Rev B 73:195123. doi:10.1103/PhysRevB.73.195123
36. Adllan AA, Corso AD (2011) Ultrasoft pseudopotentials and projector augmented-wave data sets: application to diatomic molecules. J Phys Condens Matter 23:425501. doi:10.1088/0953-8984/23/42/425501
37. Kresse G, Joubert D (1999) From ultrasoft pseudopotentials to the projector augmented-wave method. Phys Rev B 59:1758–1775
38. Swart M, Snijders JG (2003) Accuracy of geometries: influence of basis set, exchange–correlation potential, inclusion of core electrons, and relativistic corrections. Theor Chem Accounts 110:34–41. doi:10.1007/s00214-003-0443-5
39. Orita H, Itoh N, Inada Y (2004) All electron scalar relativistic calculations on adsorption of CO on Pt(1 1 1) with full-geometry optimization: a correct estimation for CO site-preference. Chem Phys Lett 384:271–276. doi:10.1016/j.cplett.2003.12.034

40. Kresse G, Furthmuller J (1996) Efficiency of ab-initio total energy calculations for metals and semiconductors using a plane-wave basis set. Comput Mater Sci 6:15–50
41. Abrahams SC, Bernstein JL (1969) Remeasurement of the structure of hexagonal ZnO. Acta Cryst B 25:1233–1236. doi:10.1107/S0567740869003876
42. Shein IR, Kiiko VS, Makurin YN, Gorbunova MA, Ivanovskii AL (2007) Elastic parameters of single-crystal and polycrystalline wurtzite-like oxides BeO and ZnO: Ab initio calculations. Phys Solid State 49:1067–1073
43. Kohout M (2011) DGRID, version 4.6. Radebeul
44. Sawada H, Wang R, Sleight AW (1996) An electron density residual study of zinc oxide. J Solid State Chem 122:148–150
45. Woll C (2007) The chemistry and physics of zinc oxide surfaces. Prog Surf Sci 82:55–120
46. Dulub O, Diebold U, Kresse G (2003) Novel stabilization mechanism on polar surfaces: ZnO(0001)-Zn. Phys Rev Lett 90:016102
47. Wander A, Schedin F, Steadman P, Norris A, McGrath R, Turner TS, Thornton G, Harrison NM (2001) Stability of polar oxide surfaces. Phys Rev Lett 86:3811–3814
48. Wander A, Harrison NM (2001) The stability of polar oxide surfaces: the interaction of H2O with ZnO(0001) and ZnO (000math). J Chem Phys 115:2312–2316. doi:10.1063/1.1384030
49. Meyer B (2004) First-principles study of the polar O-terminated ZnO surface in thermodynamic equilibrium with oxygen and hydrogen. Phys Rev B 69:045416
50. Jedrecy N, Sauvage-Simkin M, Pinchaux R (2000) The hexagonal polar ZnO(0001)-(1 x 1) surfaces: structural features as stemming from X-ray diffraction. Appl Surf Sci 162:69–73
51. King ST, Parihar SS, Pradhan K, Johnson-Steigelman HT, Lyman PF (2008) Observation of a (root 3 x root 3)R30 degrees reconstruction on O-polar ZnO surfaces. Surf Sci 602:L131–L134
52. Valtiner M, Torrelles X, Pareek A, Borodin S, Gies H, Grundmeier G (2010) In situ study of the polar ZnO(0001)-Zn surface in alkaline electrolytes. J Phys Chem C 114:15440–15447
53. Carlsson JM (2001) Electronic structure of the polar ZnO{0001}-surfaces. Comput Mater Sci 22:24–31
54. Humphrey W, Dalke A, Schulten K (1996) VMD—visual molecular dynamics. J Mol Graph 14:33–38
55. Xu PS, Sun YM, Shi CS, Xu FQ, Pan HB (2003) The electronic structure and spectral properties of ZnO and its defects. Nucl Instrum Methods Phys Res Sect B Beam Interact Mater Atoms 199:286–290
56. Kaxiras E (2003) Atomic and electronic structure of solids. Cambridge University Press, Cambridge
57. Au CT, Hirsch W, Hirschwald W (1988) Adsorption of carbon-monoxide and carbon-dioxide on annealed and defect zinc-oxide (0001) surfaces studied by photoelectron-spectroscopy (Xps and Ups). Surf Sci 197:391–401
58. Chuasiripattana K, Warschkow O, Delley B, Stampfl C (2010) Reaction intermediates of methanol synthesis and the water-gas-shift reaction on the ZnO(0001) surface. Surf Sci 604:1742–1751
59. Lindsay R, Gutierrez-Sosa A, Thornton G, Ludviksson A, Parker S, Campbell CT (1999) NEXAFS study of CO adsorption on ZnO (000(1)over-bar1)-O and ZnO (000(1)over-bar)-O/Cu. Surf Sci 439:131–138
60. Kossmann J, Rossmuller G, Hattig C (2012) Prediction of vibrational frequencies of possible intermediates and side products of the methanol synthesis on ZnO(000(1)over-bar) by ab initio calculations. J Chem Phys 136:034706. doi:10.1063/1.3671450
61. Bowker M, Houghton H, Waugh KC (1981) Mechanism and kinetics of methanol synthesis on zinc oxide. J Chem Soc, Faraday Trans 1(77):3023–3036. doi:10.1039/F19817703023